

The British University in Egypt

BUE Scholar

Centre for Advanced Materials

Research Centres

2015

A multi-scale based model for composite materials with embedded PZT filaments for energy harvesting

A.E. El-Etriby

M.E. Abdel-Meguid

K.M. Shalan

Tarek Hatem

Yehia Bahei-El-Din
ybahei@bue.edu.eg

Follow this and additional works at: https://buescholar.bue.edu.eg/centre_advanced_materials



Part of the [Computational Engineering Commons](#), [Engineering Mechanics Commons](#), [Mechanics of Materials Commons](#), [Structural Materials Commons](#), and the [Structures and Materials Commons](#)

Recommended Citation

El-Etriby, A.E.; Abdel-Meguid, M.E.; Shalan, K.M.; Hatem, Tarek; and Bahei-El-Din, Yehia, "A multi-scale based model for composite materials with embedded PZT filaments for energy harvesting" (2015). *Centre for Advanced Materials*. 6.

https://buescholar.bue.edu.eg/centre_advanced_materials/6

This Conference Proceeding is brought to you for free and open access by the Research Centres at BUE Scholar. It has been accepted for inclusion in Centre for Advanced Materials by an authorized administrator of BUE Scholar. For more information, please contact bue.scholar@gmail.com.

A MULTI-SCALE BASED MODEL FOR COMPOSITE MATERIALS WITH EMBEDDED PZT FILAMENTS FOR ENERGY HARVESTING

Ahmed E. El-Etriby¹, Mohamed E. Abdel-Meguid¹, Khalid M. Shalan¹, Tarek M. Hatem¹, Yehia A. Bahei-El-Din¹

¹ Center for Advanced Materials, the British University in Egypt, El-Shorouk City, Egypt

Keywords: Multi-scale modeling; Transformation Field Analysis; PFC; Energy Harvesting.

ABSTRACT

Ambient vibrations are major source of wasted energy, exploiting properly such vibration can be converted to valuable energy and harvested to power up devices, i.e. electronic devices. Accordingly, energy harvesting using smart structures with active piezoelectric ceramics has gained wide interest over the past few years as a method for converting such wasted energy. This paper provides numerical and experimental analysis of piezoelectric fiber based composites for energy harvesting applications proposing a multi-scale modeling approach coupled with experimental verification.

The multi-scale approach suggested predicting the behavior of piezoelectric fiber-based composites use micromechanical model based on Transformation Field Analysis (TFA) to calculate the overall material properties of electrically active composite structure. Capitalizing on the calculated properties, single-phase analysis of a homogeneous structure is conducted using finite element method. The experimental work approach involves running dynamic tests on piezoelectric fiber-based composites to simulate mechanical vibrations experienced by a subway train floor tiles. Experimental results agree well with the numerical results both for static and dynamic tests.

1. INTRODUCTION

Sources of energy surround us where a great percentage of such energy is wasted. One of these wasted sources of energy is the ambient vibrations presented from machines, ground, biological systems, etc; where embedded smart materials that are responsive

toward external stimuli can be utilized as harvesters embedded inside structures (1). These studies identified the role of adaptive smart materials in energy harvesting applications; where electrically active materials, that couple mechanical and electrical properties become of special importance for energy harvesting applications. This need has led to raising concern of piezoelectric materials as one of the promising materials for energy harvesting applications; as a result of its unique reversible process that depends on the linear interaction between the mechanical state (resulting from the applied loads) and the electrical state (extracted from ambient vibrations).

The concept behind the use of piezoelectric materials involves the combination of energy harvesting and energy storage in producing electrical energy through a direct application of the piezoelectricity concept, where the maximum power output is obtained when the frequency of the ambient vibration is closely equivalent to the resonant frequency of the vibrated structure. Piezoelectric materials in energy harvesting gained wide attention when Hausler and Stein used Polyvinylidene Fluoride film to harvest energy from ocean waves (2). Following studies by Straner, T. tackled the concept of harvesting wasted energy from daily activities (3). Among more recent studies, Elvin et al. discussed power harvesting and sensing from a strain sensor, as a PVDF film. The strain sensor was bonded to a beam in a four point bending test, where the power generated was actually enough to broadcast wireless signal of 2 meters long, in a laboratory setting, where the sensor's response was dependent on both the frequency and the applied load (4). Meninger discussed the use of a MEMS-scale variable capacitor transducer in order to convert mechanical vibrations into electrical energy for low power electronics where two harvesting methods were proposed. The first method was a voltage constrained cycle, while the second was a charge constrained cycle where it was found that a MEMS device designed to vibrate at 2520 Hz was predicted to generate a power of $8.6\mu\text{W}$ (5). Ottman et al proposed a method of increasing the harvested energy from a piezoelectric device using a step-down DC-DC converter where at lower excitations the circuit was designed to bypass the step-down converter circuit and charge the battery using the rectified piezoelectric signal as it resulted in increase of power to be 30.66 Mw (6).

In 1996 and 1997 Umeda et al. utilized an equivalent circuit model in order to predict the response of piezoelectric vibrator plate when being impacted with a steel ball inferring through simulation that maximum resistance exists for maximum power transfer from the piezoelectric layers and most of the potential energy is converted into another energy which helps the ball to rebound back off the vibrating plate leading the efficiency to decrease. Further studies that included means of rectifier and storage capacitor and an experimental design to validate the previously mentioned simulation results led to ~35% efficiency (7) and (8). In 1999, Goldfarb and Jones applied an experimental and

analytical research in order to tackle the problem of efficiency of energy harvesting of a piezoelectric generator. They had a piezoelectric stack arranged mechanically in series and electrically in parallel where this experiment resulted in maximum conversion of energy efficiency occurs at low excitation frequency less than the resonance frequency of the stack (9).

A common benchmark for energy harvesting applications use a cantilever plate subjected to base excitation (10). Initial investigations focused on the applicability of piezoelectric wafers embedded within the composite laminates. However, with recent advancements in manufacturing technology, Macro Fiber Composites (MFC) with embedded electrically active Lead Zirconate Titanate [PZT] fibers are becoming superior to monolithic wafers due to enhanced mechanical properties (11), (12) and (13).

Such composite materials are robust, in-expensive to fabricate, flexible (even in complex motion such as twisting), and have higher strength and performance than monolithic materials (14). Sodano et al investigated the vibration of similar piezoelectric composite materials both at resonant and random frequencies; it was found that the MFC materials could generate a maximum power of 2mW when reaching the resonance of the clamped plate. In addition, power was stored in both rechargeable batteries and capacitors (15). Later Sodano compared between the two different piezoelectric generators (monolithic piezoelectric materials and macro fiber composites) (16)¹ for energy harvesting applications where he investigated the ability of piezoelectric based composite materials to recharge batteries. In 2007, Farmer has introduced a thorough comparison of power harvesting techniques and its related energy storage issues (17).

On the other hand, numerical modeling of piezoelectric fiber-based composites [PFC] is mainly focused on the interpretations of overall behavior of composite-structures subjected to electrical or mechanical actuation. Analytical quantification of effective properties in active composites was subject to rigorous scrutiny. The spectrum of solutions suggested for composites with active constituents are based on expanded problems for inactive composite material, which include electro-mechanical coupling effect. Earlier models computed effective electro-mechanical properties of composite materials based on the Eshelby proposed solution for an infinite matrix with ellipsoidal inclusion (18), (19), (20) and (21). A different methodology involves asymptotic expansion homogenization techniques to extrapolate the electro-mechanical behavior of electrically active composite materials. Imposing mechanical and non-mechanical boundary conditions, a unit cell model can be used to characterize an idealized periodic geometry through the governing equations of local fields (22). Bahei-El-Din further expanded on this approach to compute the overall electro-mechanical response of electrically active woven composites using Transformation Field Analysis (TFA) while

accounting for damage progression in composite lamina (23). Incorporating the active material properties obtained from the TFA model, the dynamic behavior of the composite is evaluated as a single-phase homogenous structure with electro-mechanical behavior. A finite element method is utilized to conduct the dynamic analysis and obtain resonance frequencies of piezoelectric fiber-based composite. The proposed modeling approach verified through an experimental study conducted on PFC manufactured by Advanced Cerametrics Inc. The piezoelectric fibers are aligned unidirectional inside a resin matrix in order to provide damage tolerance for the load applied. To accurately capture the proper dynamic behavior of PFCs, piezoelectric fiber-based composite bimorph (PFCB) is used. As demonstrated in Figure 1, PFCB consists of two PFC layers bonded to a sandwiched stainless steel sheet, a bimorph piezoelectric fiber composite PFCB have a d_{33} effect along the direction of the aligned fibers.

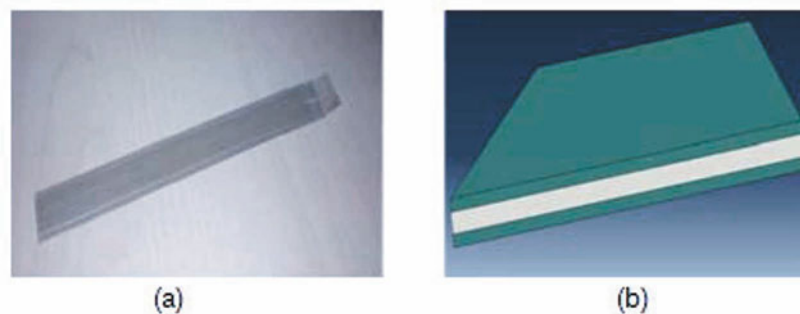


Figure 1 (a) PFC composite acquired from Advanced Cerametrics, Inc. (14), (b) Material layup of PFCBs (PFC, Stainless Steel, PFC)

2. METHODOLOGY

2.1 Piezoelectric Material

An active fiber composite (AFC) bimorph was selected to undergo the experimental analysis of the thesis. Piezoelectric Fiber Composites (PFCs) are AFCs which are manufactured by Advanced Cerametrics Inc., they are unidirectional aligned piezoelectric fibers that provide the composite with sufficient electric charge and stiffness. These fibers were manufactured carefully such that a resin matrix called epoxy surrounds the fibers in order to provide damage tolerance through load application. There are two separate interdigitated electrode layer which delivers electrical inputs and outputs. Advanced Cerametrics Inc. has conducted tests which proved that thin fibers of piezoelectric materials with a dominant dimension, length and very small cross section are capable of obtaining optimal outputs in both the direct and converse effects of piezoelectricity.

A piezoelectric fiber composite bimorph (PFCB) is used in order to increase the output power developed by inducing strain. There are two effects of piezoelectric composites which are d_{31} and d_{33} . The used type of PFCB is a bimorph piezoelectric fiber composite PFCB-W14 –having d_{33} effect. The different two types are of longitudinal and transverse piezoelectric coefficients for the rectangular piezoelectric fibers such as d_{31} and d_{33} types, respectively. Figure 2 shows the used type of PFC having an active length of the PFCB-W14 is 130mm, active width 14mm and 1.1mm thickness. According to Advanced Cerametrics Inc. the resonance frequency of the PFCB-W14 is about 27Hz (Advanced Cerametrics Inc. Piezoelectric Fiber Composites).

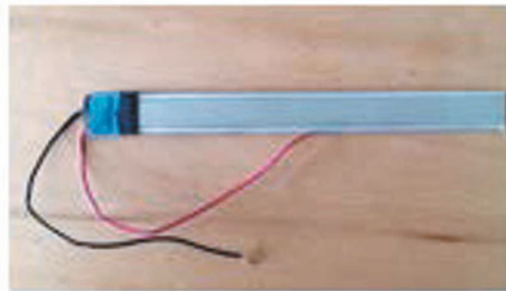


Figure 2 PFCB-W14

2.2 Numerical Modeling

The suggested computational approach discussed in this paper follow a multi-scale approach to model the electric and mechanical behavior of electrical-active -fiber embedded in a polymeric-matrix. The two stage approach consist of numerical quantification of overall electro-elastic coefficients using TFA scheme and dynamic structural analysis using ABAQUS (FEM) to model the dynamic behavior of PFCBs. Electrically induced strains in active medium is treated as transformation strains and resultant local fields and overall composite response is quantified through the TFA originally described by Dovark, G. J. (24); TFA computes the local fields using micro-geometry dependent concentrations factors, presented in Table 1. Micro-properties of composite are used to assemble the stiffness matrices in the governing equations and variable fields are solved using finite element software (25) and (26).

Table 1 Material properties of PZT-5A (23) and (26)

Type	E	ν_L	d_{33}	d_{31}	d_{15}	ϵ_{33}
------	---	---------	----------	----------	----------	-----------------

	GPa		$(\frac{m}{V} \times 10^{-12})$			$(\frac{C}{V.m} \times 10^{-9})$
PZT-5A	69	0.34	374	-171	584	15000
Epoxy	3.35	0.35	-	-	-	-

2.1.1 Constitutive Equations

Piezoelectric response can be defined through two reversible effects; first, the production of an electric field as a direct response to an applied stress; and second, a converse effect represented by mechanical deformation as a response to an applied electric potential. The linearly formulated constitutive equations binding the response of piezoelectric material are standardized by IEEE (27) . The constitutive equations for piezoelectric material are derived from the thermo-dynamical principles correlating the electric field $[E]$, strain $[S]$, stress $[T]$ and electrical displacement (28) and (29).

$$S = s^E T + dE \quad (6)$$

$$D = d^T T + \varepsilon E_k \quad (7)$$

Where, s^E is the [6x6] compliance vector for piezoelectric material, d is the [6x3] piezoelectric coupling co-efficient vector, ε is the [3x3] permittivity vector. The two equations can be symmetrically combined in matrix notation.

$$\begin{pmatrix} S \\ D \end{pmatrix} = \begin{bmatrix} s^E & d \\ d^T & \varepsilon \end{bmatrix} \begin{pmatrix} T \\ E \end{pmatrix} \quad (8)$$

Rearranging the constitutive equations for stress function

$$T = C^E S - eE \quad (9)$$

where, C^E is the [6x6] stiffness matrix

$$e = C^E d \quad (10)$$

For transversely isotropic piezoelectric material, the coefficients can be expressed in matrix notation as the following:

$$s^E = \begin{bmatrix} s_{11} & s_{12} & s_{13} & 0 & 0 & 0 \\ s_{21} & s_{22} & s_{23} & 0 & 0 & 0 \\ s_{31} & s_{32} & s_{33} & 0 & 0 & 0 \\ 0 & 0 & 0 & s_{44} & 0 & 0 \\ 0 & 0 & 0 & 0 & s_{55} & 0 \\ 0 & 0 & 0 & 0 & 0 & s_{66} \end{bmatrix} \quad (11)$$

$$d = \begin{bmatrix} 0 & 0 & 0 & 0 & d_{15} & 0 \\ 0 & 0 & 0 & d_{15} & 0 & 0 \\ d_{31} & d_{31} & d_{33} & 0 & 0 & 0 \end{bmatrix} \quad (12)$$

$$\varepsilon = \begin{bmatrix} \varepsilon_{11} & 0 & 0 \\ 0 & \varepsilon_{11} & 0 \\ 0 & 0 & \varepsilon_{33} \end{bmatrix} \quad (13)$$

Piezoelectric fiber-based composites consist of transversely isotropic ceramic piezoelectric fibers aligned in an isotropic polymer based matrix. The resultant composite material will be transversely isotropic material represented by 11 mutually exclusive coefficients representing the electro-mechanical response of the homogenized composite (25).

2.1.2 Transformation Field Analysis (TFA)

The micromechanical analysis is conducted using the TFA scheme to quantify the overall effective electro-mechanical properties of active PFC composites. Transformation field analysis represents overall response of the material through separating elastic and inelastic fields. All non-mechanical fields due to thermal or electrical actuation are considered as inelastic and treated as transformation fields, which remain in material after removing mechanical loads. The accuracy of the two-phase representation is affected by large variations in the transformation field, thus further subdivision for constituents is conducted through a Representative Volume Element [RVE]. The RVE demonstrated in **Fig. [2]** represents a single cell repeated throughout the material, which under an idealized assumption provide periodic arrangement. The unit cell used in this transformation field analysis is Periodic Hexagonal Array [PHA] (30).

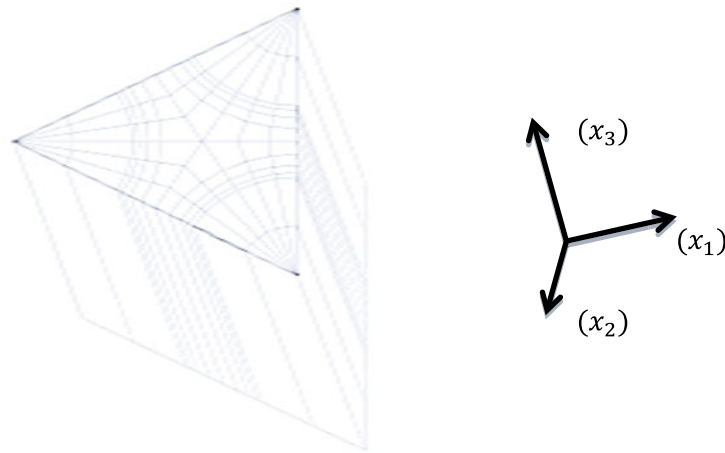


Figure 3 PHA Representative volume element employed in TFA

Eigen stresses $[\lambda]$ and strains $[\mu]$ are used to describe transformation fields for the representative volume element. Accordingly the constitutive equations for each element in an RVE can be written to incorporate induced transformation fields due to uniform stress $[T_i]$ or strain $[S_i]$.

$$S_i = s_i^E T_i + \mu_i \quad (7)$$

$$T_i = C_i^E S_i + \lambda_i \quad (8)$$

where i represent number of elements inside the RVE $[1,2\dots Q]$. Comparing equations with constitutive equations for PFC, the transformation fields can be attributed to an applied electric field in electrically active piezoelectric fiber-based composites.

$$\mu_i = d_i E_i \quad (9)$$

$$\lambda_i = -e_i E_i \quad (10)$$

For the RVE entity, the strains and stress caused by uniform stress or strain are super-positioned across the entire volume.

$$S_i = A_i S + \sum_{j=1,\Omega} D_{ij} \mu_j \quad (11)$$

$$T_i = B_i T + \sum_{j=1,\Omega} F_{ij} \lambda_j \quad (12)$$

where, Ω is the number of elements carrying transformation fields inside the RVE, and A_i and B_i are concentration factors used to describe the volume strain and stress in terms of overall counterparts. D_{ij} and F_{ij} are constant influence functions depends mainly on the elastic moduli of each element. These matrices are numerically attained through finite element analysis of the RVE under unit load and respective boundary conditions.

2.1.3 Carrera Unified Formulation

With overall properties extracted from the transformation field analysis, the extended plate theory can be used to describe the behavior of idealized composite layer. The

governing equations for piezoelectric material using PVD can be described with two variables, displacement and electric potential (31).

$$K_{uu}u + K_{u\phi}\phi = p_u - M_{uu}\ddot{u} \quad (13)$$

$$K_{\phi u}u + K_{\phi\phi}\phi = 0 \quad (14)$$

Where u, ϕ stand for the displacement vector and electric potential respectively. While the matrices K are functions of the electrical and mechanical properties of the material, for multiple layers the matrices are assembled accordingly. M_{uu}, \ddot{u} stand for the inertia matrix and the second derivative of the displacement respectively, and p_u signifies the mechanical load exerted.

The variables can be presented by using the unified formation as function of $u(x, y, z)$ and expansion functions in the z direction.

$$u(x, y, \phi) = \begin{bmatrix} u_x \\ u_y \\ \phi \end{bmatrix} \quad (15)$$

$$u(x, y, z, \phi) = \sum_{\tau=1}^Q F(z) u(x, y, \phi) \quad \tau = 1, 2, \dots, Q \quad (16)$$

The expansion functions are used to achieve higher order approximation across the thickness direction, τ signifies the order of the expansion in the z direction ranging from 1 to Q , however, in the formulation the equation can be expanded up to the fourth order. Legendre polynomials are used to express the expansion functions; their value depends on the element shape and natural coordinates.

The computation of the variables is done through a finite element model. Shape functions are used to define the relation between the nodal values and the element variable. Accordingly the equation is written as following;

$$u(x, y, z, \phi) = N_i \sum_{\tau=1}^Q F(z) q_i(x, y, \phi) \quad (17)$$

In the above equation the q describe the nodal value of the variable vector. Using the above relation the governing equation can be rearranged:

$$K_{uu}^{ijk\tau s} u^k + K_{u\phi}^{ijk\tau s} \phi^k = p_u - M_{uu} \ddot{u} \quad (18)$$

$$K_{\phi u}^{ijk\tau s} u^k + K_{\phi\phi}^{ijk\tau s} \phi^k = 0 \quad (19)$$

The subscripts i, j, τ, s are the indices used in the assembly of the stiffness matrix, where i, j and τ, s are related to the shape functions and expansion functions respectively. Subscript k indicates layer wise analysis for laminated plate structures.

2.1.4 Finite Element Modeling (FEM)

FEM approach is achieved through ABAQUS software in order to expand the scale for structural dynamic analysis (32). The electromechanical properties of the PFCBs are extracted from the micro-mechanical results of the TFA, knowing that the composite is treated as a single phase homogenous structure in the finite element model. It is vital to identify the different resonant frequencies for energy harvesting in order to avoid the improper utilization of the piezoelectric material elements. Hence, the frequency analysis is used to compute the different mode shapes of the PFCB and to compare them experimental results (25) and (26). Figure 2 shows the applied boundary conditions of the PFCB material. Numerical validation is then conducted through convergence testing in order to achieve mesh independence.

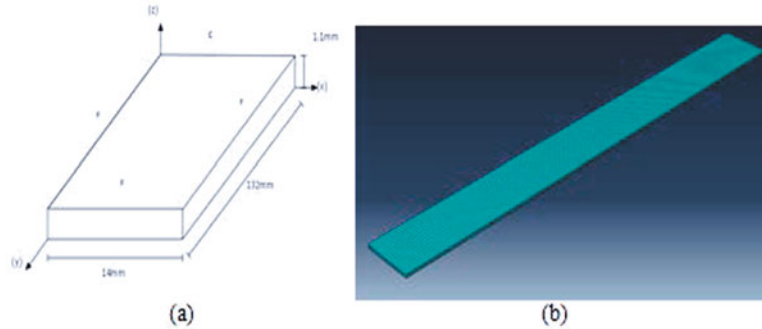


Figure 4 (a) Dimensions and mechanical constraints applied on PFC, (b) Meshed geometry using ABAQUS

3. EXPERIMENTAL ANALYSIS

This section presents an experimental analysis that validates the dynamic behavior of PFCB-W14 that was obtained by finite element modeling (FEM). The main aim of the experimental analysis is to capture the optimal voltage output versus frequency to identify the resonance occurrence during the dynamic vibration. Experimental analysis took place on two different setups targeting two different objectives. The first experimental analysis took place to investigate the behavior of the PFCB-W14 when applied to low frequencies and high amplitudes, while the other was to provide a detailed study for the sample using high frequencies and low amplitudes. The detailed study included designing a simple circuit to obtain current and power from the PFCB-W14 and determining the mechanical amplitude that is displaced by the harvester since it was

obtained in an electrical voltage. The following subsections will provide a detailed description for the two different setups and its obtained results.

3.1 Low Frequency and High Amplitude Ranges

Vibration of the PFCB-W14 took place using a universal testing machine (INSTRON 8801). The experimental setup used in this subsection is shown in Figure 3. A small steel fixture was manufactured in order to hold the sample. A steel fixture was selected due to its low damping coefficient and high strength when compared to a previously tested artilon material. Excitation of the PFCB-W14 took place through adjusting the universal testing machine to conduct the required dynamic tests for different frequency and amplitude ranging from 20-40Hz and 10-50mm respectively. Each experiment was held for 30 seconds.



Figure 5 Experimental setup for low frequency and high amplitude ranges

3.2 High Frequency and Low Amplitude Ranges

On the other hand, Figure 5 shows the complete experimental setup for high frequency and low amplitude ranges where vibration of the PFCB-W14 took place at the BUE using a V20 shaker to introduce harmonic mechanical excitation which produces 14 kHz and weighs about 15 kg, and a PA100E amplifier that produces 100W and weighs 5.5 kg (33). This amplifier is used to transfer and control the signal out from a Hameg HM8150 signal generator having a frequency range of 10mHz-12.5MHz and an output voltage of 10mVpp-10Vpp with an impedance of 50ohms (33) and (34). Figure 28 shows the previously mentioned components.



Figure 6 Experimental setup High frequency and low amplitude ranges

4. RESULTS and Discussion

4.1 Numerical Results

The dynamic modeling of the PFCBs captures the mode shapes and the corresponding resonance frequencies occurring at 24.813 Hz, 155.46 Hz, 205.79 Hz, 435.14Hz and 552.92Hz. Capturing the resonating frequencies enables proper exploitation of piezoelectric harvester as resonance is associated with maximum possible deformation of the composite structure, thus in analogy with constitutive equations achieve the maximum output voltage and current and accordingly maximum energy output. Figure 5 shows the results of the dynamic analysis.

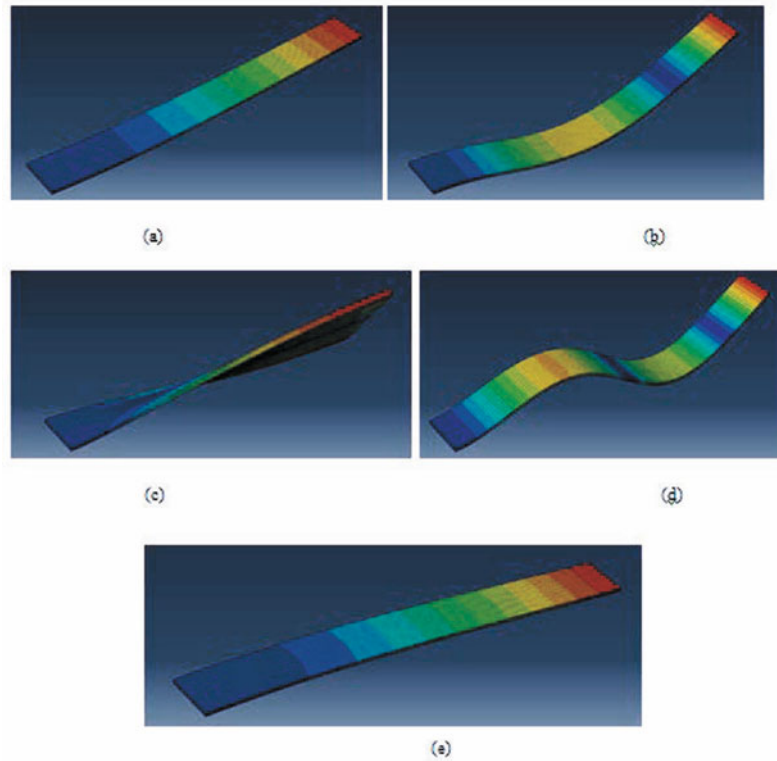


Figure 7 Five mode shapes of PFCB-W14

4.2 Experimental Results

4.2.1 Low Frequency and High Amplitude Ranges

Readings for the PFCB-W14 were tabulated at frequency ranges from 20-40 Hz and amplitude ranges from 10-50 mm for 30 seconds to identify the resonance occurrence during dynamic vibration. It was found that 20mm, 30mm and 50mm amplitudes the optimum voltage occurred at 36Hz, 23Hz and 30Hz having a value of 1.81V, 1.52V and 1.31V respectively, while for 10mm and 40mm amplitudes the optimum voltage output occurred at 28Hz having a value of 2.187V and 1.59V respectively. It was noticed that best results were obtained at 28Hz which is the same resonance frequency that were provided in the data sheet. Two comments should be added as a notice for this experimental type of experiment. The readings are of scale 1:10. The second comment is that the universal testing machine represents a large percentage of error which resulted in obtaining higher maximum voltage at lower amplitude. This error was investigated and was solved in the second experimental setup when using an electromagnetic shaker having high frequency and low amplitude ranges.

Figure 7 shows the best obtained voltage versus frequency according to both the datasheet provided from Advanced Cerametrics Inc. and the FEM where resonance

frequency occurred at 28Hz and 24.813Hz respectively (Advanced Cerametrics Inc. Piezoelectric Fiber Composites). The best voltage value peaks at 28Hz for 10mm and 40mm amplitudes which mean that the numerical modeling provides an adequate approximation to the resonance of the PFCB-W14.

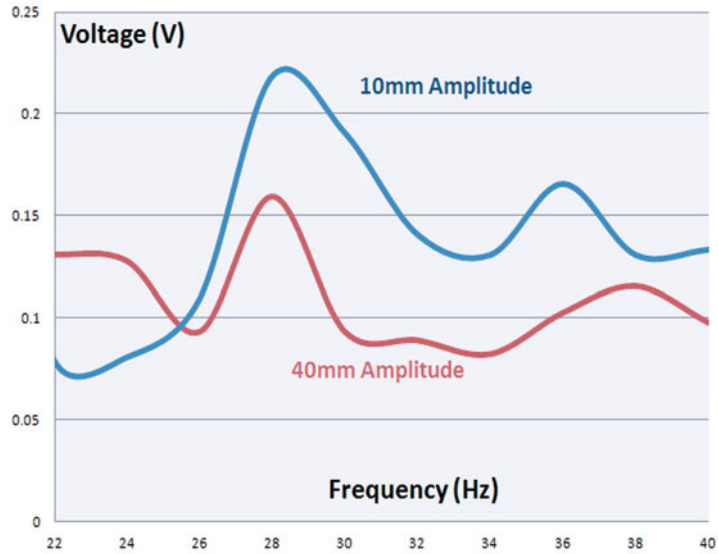


Figure 8 Resonance Frequency determined to be 28 Hz at 10mm and 40mm amplitudes

4.2.2 High Frequency and Low Amplitude Ranges

Readings for the PFCB-W14 were tabulated at frequency sweep of 10-200Hz at electrical amplitude of 100V_{rms} for 100 seconds to identify the first two modes of shape of the piezoelectric material during dynamic vibration. Figure 8 shows that the optimum output voltage obtained when no resistance was added 8.5V_{rms} and 5.02V_{rms} at 20.25Hz and 143.79Hz respectively. There is noise presented at 1Hz and 60Hz and this resembles a pick up voltage with other signals inside the vibration lab.

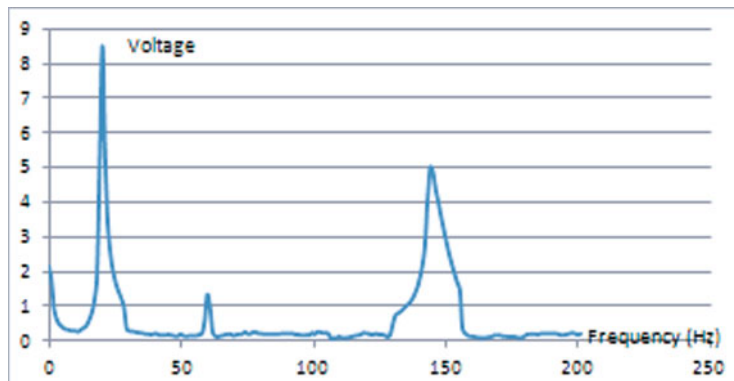
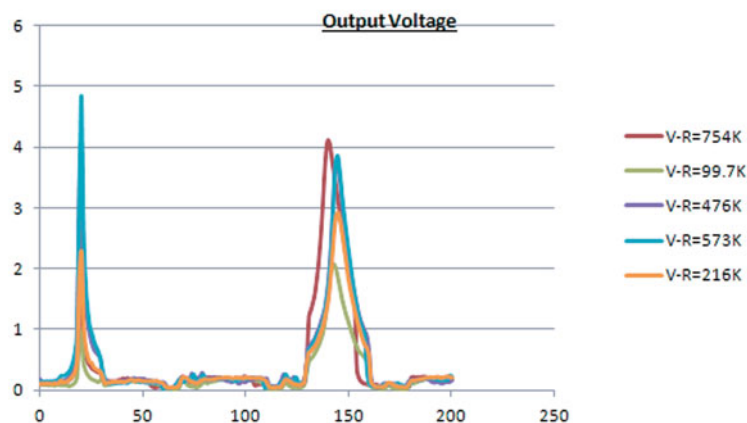


Figure 9 Obtained 1st and 2nd modes of shape when no resistance was added

In order to obtain current and power, a circuit design with different resistances was essential. Knowing that the internal resistance is effective only in case of adding an external resistance, another experiments were conducted since the voltage value will change. When adding a resistance of 99.7Kohm, a 0.976V, 0.0098mA and 0.096mW was obtained at 19.23Hz which resembles the first mode shape, and 2.06V, 0.021mA and 0.0427mW at 142.7Hz which resembles the second mode shape. It is important to note that when adding a 99.7Kohm resistance it decreases the voltage and current of the first mode shape dramatically leading to the obvious appearance of noise. A higher resistance of 216Kohm was added in order to investigate the changes of voltage, current and power. A 216Kohm has led to the occurrence of 2.28V, 0.0083mA and 0.024mW at 20.25Hz as a first mode shape, and 2.94V, 0.0136mA and 0.03988mW at 144.7Hz as a second mode shape. Another higher resistance was added, where it was found that at 476Kohm voltage, current and power take place at 4.077V, 0.0086mA and 0035mW respectively at 20.25Hz for the first mode shape. While at 144.7Hz for the second mode shape, voltage, current and power take place at 3.75V, 0.0079mA and 0.0295mW respectively. A 537Kohm resistance was used where it was obtained at 19.24Hz as a first mode shape having a voltage, current and power of 4.077V, 0.0086mA and 0.041mW respectively. While at 144.7Hz a voltage of 3.85V, current of 0.0068mA and power of 0.0261mW was obtained. It was observed that when adding 537Kohm voltage and power of second mode shape is slightly lower than that of the first mode shape. Finally first mode shape was obtained at 20.25Hz, while second mode was obtained at 139.7Hz when adding a resistance of 754Kohm. For the first mode shape voltage, current and power occurs at 2.787V, 0.0037mA and 0.01mW, while for the second mode shape voltage, current and power occurs at 4.11V, 0.0055mA and 0.0224mW respectively. Figure 9 shows all the obtained values for the voltage, power and current.



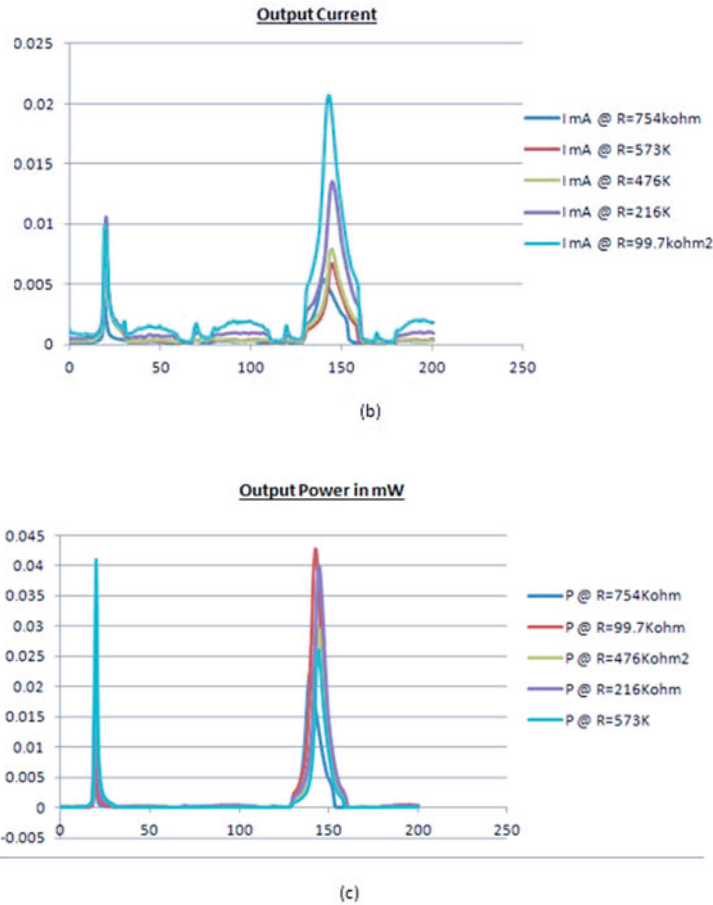


Figure 10 Obtained voltage, current and power using different values of resistors respectively

5. CONCLUSION

In the current study a multi-scale approach been utilized to extract the behavior of composite structures with electrically active fibers. The model demonstrated proper approximation of the experimental results. Both models, the micro-scale (TFA) model and macro-scale model (FEM), been successfully utilized through a hierarchal approach; accuracy is increased substantially with fiber-fiber interaction scheme of the TFA in micro-scale and the structural response in macro-scale. Extracting the electro-mechanical properties of the composite material from the micro-mechanical model allows a significant reduction in the computational cost at the macro-scale and therefore enables the modeling of more complex geometry and structures utilizing the proposed multi-scale approach. Experimental analysis on PFCBs indicates that the multi-scale model present

proper representation of the dynamic behavior associated with PFCs, thus this model can be expanded toward energy harvesting devices that efficiently capture dynamic energy.

Future work is presented in energy harvesting using piezoelectric materials to convert the mechanical strain induced inside the trains into electric charges to empower the train's light. A simple schematic 3D drawing was created using Solidworks in order to create a preliminary imagination for the model. The model consists of three patches of piezoelectric materials connected together in parallel connections since this produces higher output, shown in Figure 10. These patches are mounted on a floor which is beneath it a spring that is mounted on the main floor of the train. This model is supposed to vibrate due to the motion of the crowd inside the train or due to the train motion.

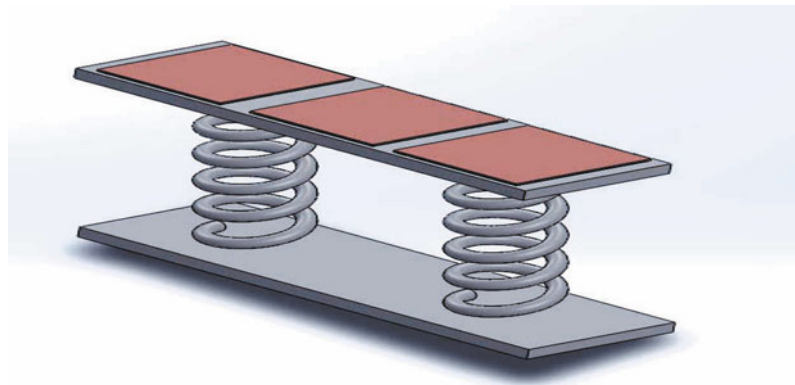


Figure 11 Preliminary model for achieving the future work

Bibliography

1. *Review of State of Art of Smart Structures and Integrated Systems*. Chopra, Inderjit. s.l. : AIAA, 2002, AIAA, pp. 2145-2187.
2. *Hydromechanical and Physiological Mechanical - to - Electrical Power Converter with PVDF*. Hausler, E. and Stein, L. s.l. : Ferroelectrics, 1987, pp. 363-369.
3. *Human Power Wearable Computing*. Starner, T. s.l. : IBM System, 1996, pp. 618-629.
4. *A Self-Powered Mechanical Strain Energy Sensor*. Elvin, N., Elvin, A. and Spector, M. 2001. *Smart Materials and Structures*. pp. 293-299.

5. *Vibration - to - Electric Energy Conversion*. Meninger, S, et al. s.l. : IEEE, 2001. IEEE Transactions on Very Large Scale Intergration. Vol. 9, pp. 64-67. 1.
6. *Optimized Piezoelectric Energy Harvesting Circuit Using Step Down Converter in Discontinuous Conduction Mode*. Ottman, G., Hofmann, H. and Lesieutre, G. s.l. : IEEE, 2002. Proceedings of IEEE 33rd Conference of Annual Power Electronics Specialists.
7. *Analysis of the Transformation of Mechanical Impact of Energy to Electric Energy Using Piezoelectric Vibrator*. Umeda, M., Nakamura, K. and Ueha, S. 1996, Japanese Journal of Applied Physics, pp. 3267-3273.
8. *Energy Storage Characteristics of a Piezo-generator Using Impact Induced Vibration*. Umeda, M., Nakamura, K. and Ueha, S. 1997, Japanese Journal of Applied Physics, pp. 3146-3151.
9. *On the Efficiency of Electric Power Generation with Piezoelectric Ceramic*. Goldfarb, M. and Lowell, D. 1999, Dynamic Systems, Measurement and Control, pp. 566-571.
10. Ertruk, A. and Inman, A. *Piezoelectric Energy Harvesting*. 2011.
11. *Anisotropic Actuation with Piezoelectric Fiber Composites*. Hagood, A. A., Rodgers, N. W. and Bent, J. P. 1995, Intelligent Material Systems and Structures, Vol. 6, pp. 337-349.
12. *An overview of Composite Acutators with Piezoceramics*. Williams, R. Brett, et al. 2002. in Proceeding of IMAC XX. pp. 421-427.
13. *Modeling 1-3 Composite Plezoelectrics: Thickness-Mode Oscillations*. Smith, W. A. and Auld, B. A. 1991, Ultrasonics, Feroelectrics, and Frequency Control, Vol. 38, pp. 40-47.
14. Advanced Cerametrics Inc. Piezoelectric Fiber Composites. [Online] <http://www.advancedcerametrics.com/products/energy-harvesting/piezoelectric-fiber-composites/>.
15. *Electric Power Generation from Piezoelectric Materials*. Sodano, H., et al. 2002. The 13th Internation Conference on Adaptive Structures and Technologies.
16. *Use of Piezoelectric Energy Harvesting Devices for charging Batteries*. Sodano, H., et al. s.l. : SPIE, 2003. SPIE 10th Annual International Symposium on Smart Structures and Non Destructive.
17. Farmer, J. *A Comparison of Power Harvesting Techniques and Related Energy Storage Devices*. s.l. : Masters of Science in Mechanical Engineering, Virginia Polytechnic Institute and State University, 2007.
18. *The determination of the elastic field of an ellipsoidal inclusion, and related problems*. Eshelby, J. D. 1957. Royal Society of London. pp. 376-396.

19. *Micromechanics Predictions of the Effective Electroelastic Moduli of Piezoelectric Composites*. Dunn, M. L. and Taya, M. 1993, International Journal of Solids and Structures, pp. 161-175.
20. *Micromechanics of Magneto-electroelastic Composite Materials: Average Fields and Effective Behaviour*. Li, Jiang Yu and Dunn, Martin L. 1998. Intelligent Material Systems and Structures. pp. 404-416.
21. *Average stress in matrix and average elastic energy of materials with misfitting inclusions*. Mori, T and Tanaka, K. 1973. Acta Metallurgica. pp. 571-574.
22. *Numerical Evaluation of Effective Material Properties of Transversely Randomly Distributed Unidirectional Piezoelectric Fiber Composites*. Kari, Sreedhar, et al. 2007. Intelligent Material Systems and Structures. pp. 361-371.
23. *Modelling electromechanical coupling in woven composites exhibiting damage*. Bahei-El-Din, Y. A. 2009. Aerospace Engineering. pp. 485-495.
24. *Transformation field analysis of inelastic composite materials*. Dvorak, G. J. 1992. Proceeding of Royal Society. pp. 311-327.
25. *A Multiscale-Based Approach for Composite Materials with Embedded PZT Filaments for Energy Harvesting*. El-Etriby, Ahmed, et al. San Diego : SPIE, 2014. Smart Structures and Non Destructive Evaluation.
26. *"MULTISCALE MODEL AND EXPERIMENTAL STUDY OF DAMAGE IN PIEZOELECTRIC FIBER-BASED COMPOSITE*. Shalan, K., et al. 2014. European Workshop on Structural Health Monitoring (EWSHM).
27. Institute of Electrical and Electronics Engineers Standard on Piezoelectricity. *Std 176 IEEE* . s.l. : ANSI/IEEE, 1987.
28. *Classical and Advanced Theories for Modelling and Analysis*. Carrera, Erasmo. Torino : s.n., 2008, Plates and Shells for Smart Structures, p. Wiley.
29. *Fundamentals of Piezoelectricity*. Ikeda, T. 1996, Oxford University Press.
30. Teply, J. *Periodic Hexagonal Array Models for Plasticity Analysis of Composite Materials*. 1984.
31. Carrera, E. *Plates and Shells for Smart Structures: Classical and Advanced Theories for Modelling and Analysis*. Torino : Wiley, 2008.
32. Simulia. *ABAQUS 6.10 Documentation*.
33. *Signal Force Data Physics*. s.l. : Data Physics.
34. *HAMEG Instruments*.